lubricants

MDPI

Article

Stability and Thermal Conductivity of Mono and Hybrid Nanoparticles Dispersion in Double-End Capped PAG Lubricant

Mohd Zaki Sharif [1], Wan Hamzah Azmi [1,2,*], Mohd Fairusham Ghazali [1], Nurul Nadia Mohd Zawawi [1] and Tri Yuni Hendrawati [3]

[1] Centre for Research in Advanced Fluid and Processes, Lebuhraya Tun Razak, Kuantan 26300, Pahang, Malaysia
[2] Faculty of Mechanical and Automotive Engineering Technology, Universiti Malaysia Pahang, Pekan 26600, Pahang, Malaysia
[3] Department of Chemical Engineering, Universitas Muhammadiyah Jakarta, Jl. Cempaka Putih Tengah 27, Jakarta 10510, Indonesia
* Correspondence: wanazmi@ump.edu.my; Tel./Fax: +60-19-6575876

Abstract: Stable nanolubricant mixtures are interrelated with thermal conductivity enhancement, thus improving heat transfer performance in automotive air conditioning (AAC) systems. This paper studies the stability and thermal conductivity of double-end capped polyalkylene glycol (PAG)-based nanolubricants specially designed for R1234yf refrigerant. Mono nanolubricants (Al_2O_3/PAG and SiO_2/PAG) and hybrid nanolubricants (Al_2O_3–SiO_2/PAG) were prepared using a two-step preparation method at different volume concentrations of 0.01 to 0.05%. The stability of these nanolubricants was observed by visual, UV-Vis spectrophotometer, and zeta potential. Thermal conductivity (k) was measured from 30 to 70 °C using a C-Therm thermal properties analyser. The results from the stability analysis show that all nanolubricants were confirmed in excellent stability conditions for more than six months with minimum visual sedimentation, more than 70% concentration ratio, and zeta potentials greater than 60 mV. The Al_2O_3–SiO_2/PAG samples recorded the highest values of thermal conductivity increment, followed by the Al_2O_3/PAG and SiO_2/PAG samples with 2.0%, 1.7%, and 1.5% enhancement. Hybrid nanolubricants have been shown to have greater potential in the AAC system because of their excellent stability and better property enhancement in thermal conductivity.

Keywords: hybrid nanolubricants; stability; thermal conductivity; double end-capped PAG; refrigeration system

Citation: Sharif, M.Z.; Azmi, W.H.; Ghazali, M.F.; Zawawi, N.N.M.; Hendrawati, T.Y. Stability and Thermal Conductivity of Mono and Hybrid Nanoparticles Dispersion in Double-End Capped PAG Lubricant. *Lubricants* **2023**, *11*, 1. https://doi.org/10.3390/lubricants11010001

Received: 29 November 2022
Revised: 15 December 2022
Accepted: 16 December 2022
Published: 20 December 2022

1. Introduction

Hydrofluoroolefins (HFO) R1234yf has been suggested as an excellent drop-in replacement for R134a because it has a low global warming potential (GWP). However, performance analysis of R1234yf (2,3,3,3-Tetrafluoroprop-1-ene) and R1234ze(E) (trans-1,3,3,3-Tetrafluoropropene) on the existing vapour-compression system observed a marginal reduction in the coefficient of performance (COP) compared to R134a (1,1,1,2-Tetrafluoroethane) [1]. Thus, increasing the efficiency of the automotive air conditioning (AAC) system can reduce fuel or energy consumption, emissions, and environmental problems. Improvements must be made to the AAC system's performance because it is one of the parasitic loads on an automobile engine. Therefore, using the appropriate working fluids will be required to improve the efficiency of the AAC system. As suggested by a review study, one of the potential solutions is to improve the thermal performance of heat transfer fluids in AAC by using nanolubricants [2]. Inspired by the study of effective thermal conductivity by Masuda et al. [3] and Choi and Eastman [4], nanotechnology-based lubricants have been thoroughly researched to improve the thermal performance of conventional lubricants [5,6].

It is not recommended for the R1234yf refrigeration system to use the existing PAG lubricant, which is currently used for R134a. PAG is produced by reacting alkylene oxide monomers with a nucleophilic starter, often alcohol [7]. R1234yf is more sensitive than R134a and interacts more readily with water and oil. Excessive moisture will react with the oil and refrigerant, thus producing an acid reaction and therefore harming the compressor. A new, nonhygroscopic, double-ended capped PAG lubricant blend should be used and have protection against moisture. Double-ended capped oil has the main chemical chain closed on both sides, whereas single-ended capped oil has the main chemical chain closed on just one side [8]. The single-end capped PAG still has a functional hydroxyl group (–OH) chain at the other end; therefore, it is chemically unstable and tends to attract other substances [9]. While the double-end capped ND-oil 12 is unreactive, more stable, and resistant to moisture, it maintains the maximum degree of lubricating performance throughout time. So far, some compressor lubricant manufacturers have released several versions of lubricants for AAC systems using R1234yf, such as PAG PAG ND12 (Denso) and PAG SP-A2 (Sanden), and PAO AA1 (Mahle). Much research has been conducted to study the effects of nanoparticles incorporated into PAG compressor lubricants designed for the AAC-R134a system. Sharif et al. [10] studied the thermal conductivity and viscosity of 0.05 to 1.0% of Al_2O_3/PAG for the R134a system over the temperature range of 30 to 70 °C. The thermal conductivity enhancement ratio was 1.04 at 1% volume concentration. Their result shows that the thermal conductivity of the nanolubricants over the base fluid increases with the increase in particle concentration and temperature. In addition, the thermal conductivity decreased with an increase in temperature. Sanukrishna and Jose Prakash [11] investigated the thermal conductivity of TiO_2/PAG nanolubricants over the temperature range of 20 to 50 °C at various particle volume concentrations up to 0.8%. The thermal conductivity enhancement of TiO_2 nanolubricants compared to pure PAG is 37.8% at 20 °C with a volume concentration of 0.8%. The same author repeated the experiment using SiO_2/PAG in another study [12]. The volume concentration tested was from 0.07 to 0.6% over an extended temperature range of up to 50 °C. Both studies concluded that the thermal conductivity-temperature behaviour of the nanolubricants closely followed the behaviour of the base fluid, with a noticeable enhancement. The maximum enhancement in thermal conductivity ratio obtained by SiO_2/PAG nanolubricants was 1.31 at a volume fraction of 0.6% and a temperature of 20 °C. It is expected that TiO_2/PAG nanolubricants have a higher increment than Al_2O_3/PAG and SiO_2/PAG since the nanoparticles TiO_2 have a higher thermal conductivity than Al_2O_3 and SiO_2 when it is dispersed inside the fluid. [13]. The improvement in thermal conductivity seen in the experiment exceeds all predictions made by classical models. This may be because all classical models are based on liquids with low viscosity, such as water, ethylene glycol, etc. However, the study by Sanukrishna and Jose Prakash [11] did not report any stability data, which are an essential factor.

Typically, hybrid nanolubricants have a minor increase in viscosity and a significant increase in heat conductivity. Zawawi et al. [14] investigated the thermo-physical properties of Al_2O_3–SiO_2 and Al_2O_3–TiO_2 hybrid nanolubricants. The highest thermal conductivity enhancement was 2.41% for Al_2O_3–SiO_2 nanolubricants, while maximum viscosity increments of 20.50% were obtained for Al_2O_3–TiO_2 nanolubricants. The high potential of the Al_2O_3–SiO_2 combination may be attributable to its stability in the PAG, leading to a good improvement in heat conductivity with a low viscosity increase. Later, in the study undertaken by Zawawi et al. [15], it was concluded that Al_2O_3–SiO_2/PAG nanolubricants with a nanoparticle ratio of 60:40 and volume concentrations of less than 0.1% are highly recommended for application in the refrigeration system. This means that the nanoparticle ratio in hybrid nanolubricants also plays an essential role in the thermo-physical properties of nanolubricants. Comparing the impact of surfactant addition and ultrasonic processing, Ghadimi et al. [16] investigated the stability of titania nano-suspensions. The findings show that a 180 min ultrasonic bath method with the addition of 0.1% surfactant may produce the most stable suspension with the best thermal conductivity for use within one month.

Occasionally, the thermal conductivity of the nanofluid will rise if the improvement in stability is followed by ultrasonication and the addition of a suitable surfactant [16,17].

Previous studies focused solely on the characteristics of PAG-based nanolubricants for AAC-R134a. To date, the research on the properties of nanolubricants has been focused on PAG for R134a systems [5,11,12]. Apart from that, several studies have also been conducted to investigate the addition of nanoparticles into refrigerants or lubricant mixtures to improve refrigeration systems' performance [6]. Studies on the double-end capped PAG/nanoparticle mixture intended for AAC-R1234yf are scarce. Additionally, the investigation of nanolubricants in PAG lubricants for the AAC-R1234yf system regarding their effect on stability and thermal conductivity has yet to be reported in the literature. Thus, in the present study, a systematic investigation of stability and thermal conductivity of Al_2O_3/PAG, SiO_2/PAG (mono nanolubricants), and Al_2O_3–SiO_2/PAG (hybrid nanolubricants) were conducted to evaluate the applicability of the new type of polyalkylene glycol (PAG ND12) nanolubricants for the AAC-R1234yf system. A systematic stability evaluation procedure was performed by finding the best sonication time and an extensive stability evaluation [18]. Novel thermal conductivity correlations were proposed to estimate the thermal conductivity of Al_2O_3/PAG, SiO_2/PAG, and Al_2O_3–SiO_2/PAG hybrid nanolubricants, mainly for application in automotive air-conditioning (AAC) compressor systems.

2. Experimental Methodology

2.1. The Materials Specification

Nanolubricants are prepared by dispersing nano-sized particles into a conventional lubricant using a two-step preparation method. Prior to this, however, a number of factors must be taken into account: shape, size, thermal conductivity, cost, and stability [19]. Al_2O_3 and SiO_2 nanoparticles are among the suitable nanoparticle materials used in lubricants in the AAC system. The lower cost of Al_2O_3 and SiO_2 is preferable for mass production [20,21]. Al_2O_3 nanoparticles are known not to be susceptible to surface oxidation and are much easier to incorporate into a fluid [22]. This explains why Al_2O_3-based nanolubricants have excellent stability, especially in lubricants [10,15].

Moreover, Al_2O_3 and SiO_2 nanoparticles have better tribological properties due to low friction coefficient and better anti-wear properties [23,24]. The friction reduction in nanolubricants can be attributed to the ability of nanoparticles to transform sliding friction into rolling friction (nanoparticle mechanism) due to the reduced interfacial frictional surface action caused by the presence of nanoparticles between contact surfaces [25]. Although the thermal conductivity of Al_2O_3 and SiO_2 is not as high as that of other metal oxide materials such as CuO and ZnO, these nanoparticles are steadily gaining ground in the AAC system due to their smaller size and stability. This is because the AAC system uses a stable lubricant due to its widespread use in vehicles. Al_2O_3 (99.8%) metal oxides and SiO_2 (99.8%) acidic oxides nanoparticles used in this study were procured from Sigma-Aldrich (St. Louis, MO, USA) and Beijing Deke Daojin Science & Technology Co. Ltd. (Beijing, China), respectively. Both nanoparticles have mean particle sizes of 13 and 30 nm, as the manufacturer's specifications provide. While PAG ND12, acquired from DENSO, was used as the base lubricant. PAG ND12 is a lubricant formulated for R1234yf and R134a in the vapour compression system. Tables 1 and 2 provide the properties of the present nanoparticles and the base lubricant, respectively.

Table 1. Properties of Al_2O_3 and SiO_2 nanoparticles.

Property	Unit	Al_2O_3	SiO_2
Average particle diameter	nm	13	30
Density	$kg{\cdot}m^{-3}$	4000	2220
Purity	%	99.9	99.9
Molecular mass	$g(mol)^{-1}$	101.96	60.08
Specific heat	$J(kg{\cdot}K)^{-1}$	773	745
Thermal Conductivity	$W(m{\cdot}K)^{-1}$	36	1.4

Table 2. Chemical and physical properties of the double end-capped PAG ND12 lubricant.

No.	Properties	Value
1	ISO viscosity grade	46
2	Kinematic viscosity at 40 °C	39.3 cP
3	Kinematic viscosity at 100 °C	8.45 cP
4	Viscosity index	216.157
5	Density at 40 °C	1.021 g(cm)$^{-3}$
6	Density at 100 °C	0.976 g(cm)$^{-3}$
7	Flash point	−36 °C

2.2. Nanolubricants Characterisation and Stability Evaluation

The Al_2O_3/PAG, SiO_2/PAG, and Al_2O_3–SiO_2/PAG were prepared at a volume concentration of 0.01 to 0.05%. The Al_2O_3–SiO_2/PAG hybrid nanolubricants ratio was prepared at a ratio of 80:20. The 80:20 ratio for hybrid nanolubricants was chosen for the characterisation process because it was proven that this ratio gave the best performance in the AAC-R1234yf system in previous experiments [26]. The mass of nanoparticles required for each sample was calculated using a nanoparticle volume concentration formula that has been derived from previous studies [27]. The base lubricant and nanoparticles were combined with a magnetic stirrer to create each sample over 30 min. A high-frequency ultrasonic water bath (FisherbrandTM Advanced Ultrasonic Bath) was then used to further homogenise it in order to break the bond between the nanoparticles. During the sonication process, the ultrasonic water bath frequency and power are kept constant at 37 Hz and 80 W. A schematic diagram of nanoparticle-stabilized oil droplets in PAG lubricant oil is shown in Figure 1. The four steps of analysis for the spectral absorbency analysis were performed in this investigation by following previous recommendations [18]. For the best nanolubricants stability, the ideal ultrasonic sonication time was examined to determine the optimum process duration. It is crucial to produce stable nanolubricants with a minimum time to improve the efficiency of the whole experimental routine. Therefore, an investigation was conducted to find the optimum sonication time to achieve the most stable nanolubricants.

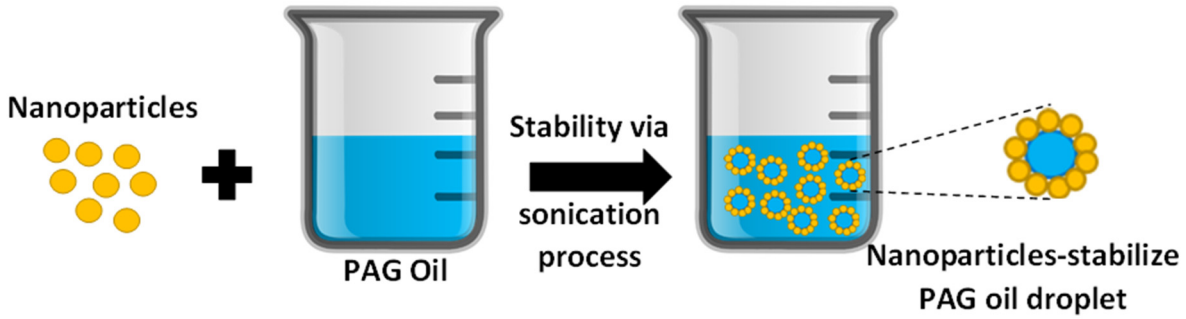

Figure 1. Schematic diagram of nanoparticle-stabilized oil droplets in PAG lubricant oil.

Transmission electron microscopy (TEM) is used to detect the average size, shape and condition of nanoparticles suspended in a nanolubricant dispersion. A cross-sectional photograph taken through a microscope image usually shows the state of dispersion of nanoparticles in PAG lubricants at a high magnification scale. Average size and shape can also be estimated using the cross-sectional image. A portion of the prepared sample was put into a test tube for visual observation. The visual condition of the sample was observed by comparing the deposition of the sample under the test tube over a period of time. The visual comparison of the sample was compared with the difference in volume concentration and the type of nanoparticles.

Ultraviolet–Visible (UV-Vis) spectral absorbency analysis method was used to evaluate the dispersion stability of nanolubricants for a more extended period. Spectral absorption analysis was performed using a UV-Vis spectrophotometer (Thermo Scientific GENESYS

30, Thermo Scientific, Waltham, MA, USA) to measure the variation in concentration or the absorbance (A) of the supernatant particles with sediment time. The decrease in concentration ratio indicates that particle deposition has occurred on the sample. According to Beer's law [28], the particle concentration in the nanofluid has a linear relationship with the light absorbance of the nanofluid.

The nanoparticle's surface charge (zeta potential) and average aggregate size were measured by a particle analyser (Litesizer 500 Anton Paar Particle size analyser, Graz, Austria) based on the electrophoretic light scattering technique. The zeta potential study aims to measure the repulsive force between particles. An adequate repulsive force can help overcome the natural attraction between particles. This is to prevent particles from agglomerating. The zeta potentials of 0.01% volume concentration of Al_2O_3/PAG, SiO_2/PAG, and Al_2O_3–SiO_2/PAG nanolubricants.

2.3. Thermal Conductivity Measurement

In this study, the C-Therm TCi Thermal Conductivity Analyzer was used to measure the thermal conductivity of the nanolubricants. The C-Therm apparatus design consists of a computer, data acquisition hardware, and a sensor. The sensor probe for this device consists of a single-sided, interfacial heat reflectance sensor that applies a momentary constant heat source to the sample. This device employs a modified transient plane source and transient line source methods, which comply with ASTM D7984, ASTM D5334, D5930, and IEEE 442-1981. It is designed primarily to measure thermal conductivity from 0 to 500 W/m.K with an accuracy of $\pm$0.001 W/m.K.

A nanolubricants sample of 1.5 mL was measured in the small-volume liquids test cell. A heating oven was used to maintain a constant temperature of the sample with an accuracy of 0.1 °C. Electric current was supplied through the device and through the system from time to time. Heat is applied to the sensor to heat the sample, and the temperature is monitored inside the small-volume liquid test cell. The corrections were undertaken to account for the temperature drift and estimate the thermal conductivity. This software calculates the thermal conductivity and stores the thermal conductivity data inside the computer. At least five measurements were taken for each concentration at a specific temperature to ensure the measurement was within $\pm$5% accuracy. The sensor was validated by determining the thermal conductivity of the verification liquid (distilled water). The measured value for distilled water at a temperature of 30 °C was 0.604 W/m.K, which was in agreement with the calibrated data of 0.6145 W/m.K and within $\pm$5% accuracy. The sensor was validated each time before the measurement of thermal conductivity.

3. Results and Discussion

3.1. Characterisation and Stability Evaluation

3.1.1. Sonication Time Evaluation

The SiO_2/PAG, Al_2O_3/PAG, and Al_2O_3-SiO_2/PAG nanolubricants were prepared at a constant 0.01% volume concentration. The nanolubricants were prepared at different sonication times, from zero to 180 min, with 60 min intervals. The peak wavelengths for all samples were noted at 306 nm for all nanolubricants, according to the UV-Vis absorption scanning from 200 to 900 nm, as shown in Figure 2. The wavelength at this point offers the highest absorbance value. At a constant wavelength of, on average, 306 nm throughout the experiment, the colloidal stability of each sample was assessed. From the UV-Vis absorbance experiment, the Al_2O_3/PAG nanolubricant has the maximum absorbance, followed by the Al_2O_3-SiO_2/PAG and SiO_2/PAG nanolubricants. The results demonstrate that the nanolubricant sample with the whitest colour is Al_2O_3/PAG and followed by Al_2O_3-SiO_2/PAG. Typically, the colourless SiO_2 nanoparticles diminish the white colour for the Al_2O_3-SiO_2/PAG nanolubricant; thus, the peak absorbance value also decreases. Beer's law was used to demonstrate a linear relationship between nanolubricants absorption and volume concentration. The linear relationship between concentration and absorption for SiO_2/PAG, Al_2O_3/PAG, and Al_2O_3-SiO_2/PAG nanolubricants is depicted in Figure 3. The

graph depicts a linear relationship between volume concentration and absorbance. For a particular absorbance value, this line may predict an unknown volume concentration of nanolubricants. The higher absorbance indicated higher volume concentrations of suspended nanoparticles. The results from Figure 3 are crucial for validating the information in the following Figure 4.

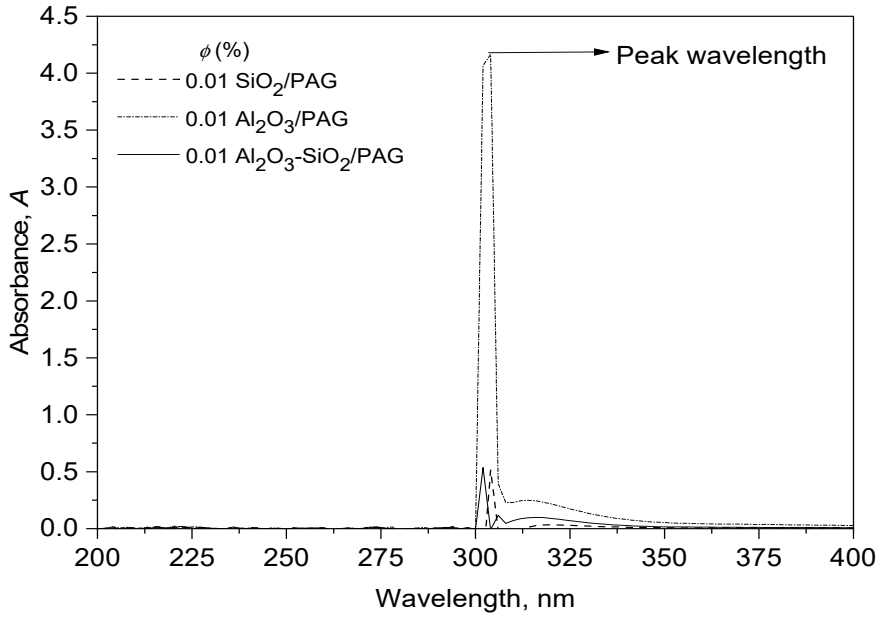

Figure 2. Absorbance of nanolubricants at a different wavelength.

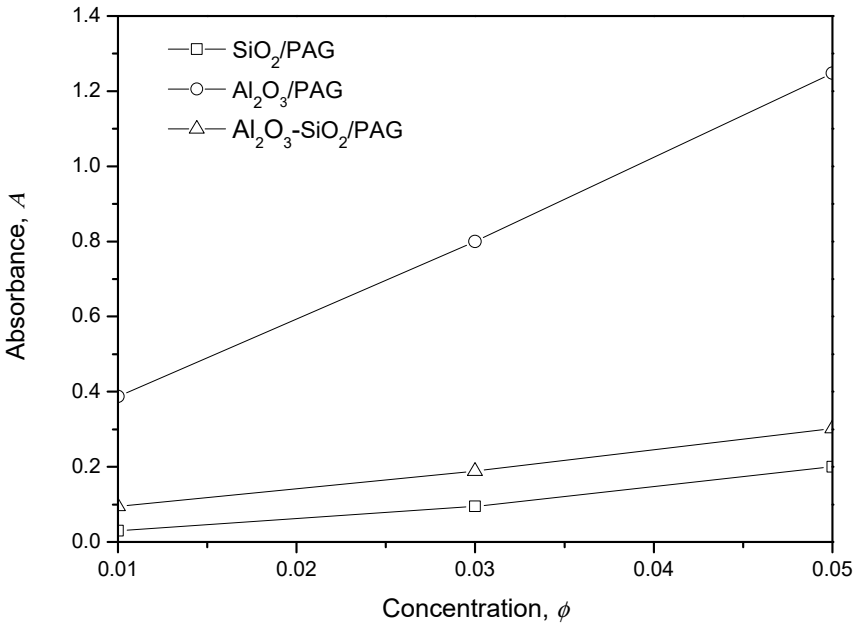

Figure 3. Absorbance of nanolubricants at different volume concentrations.

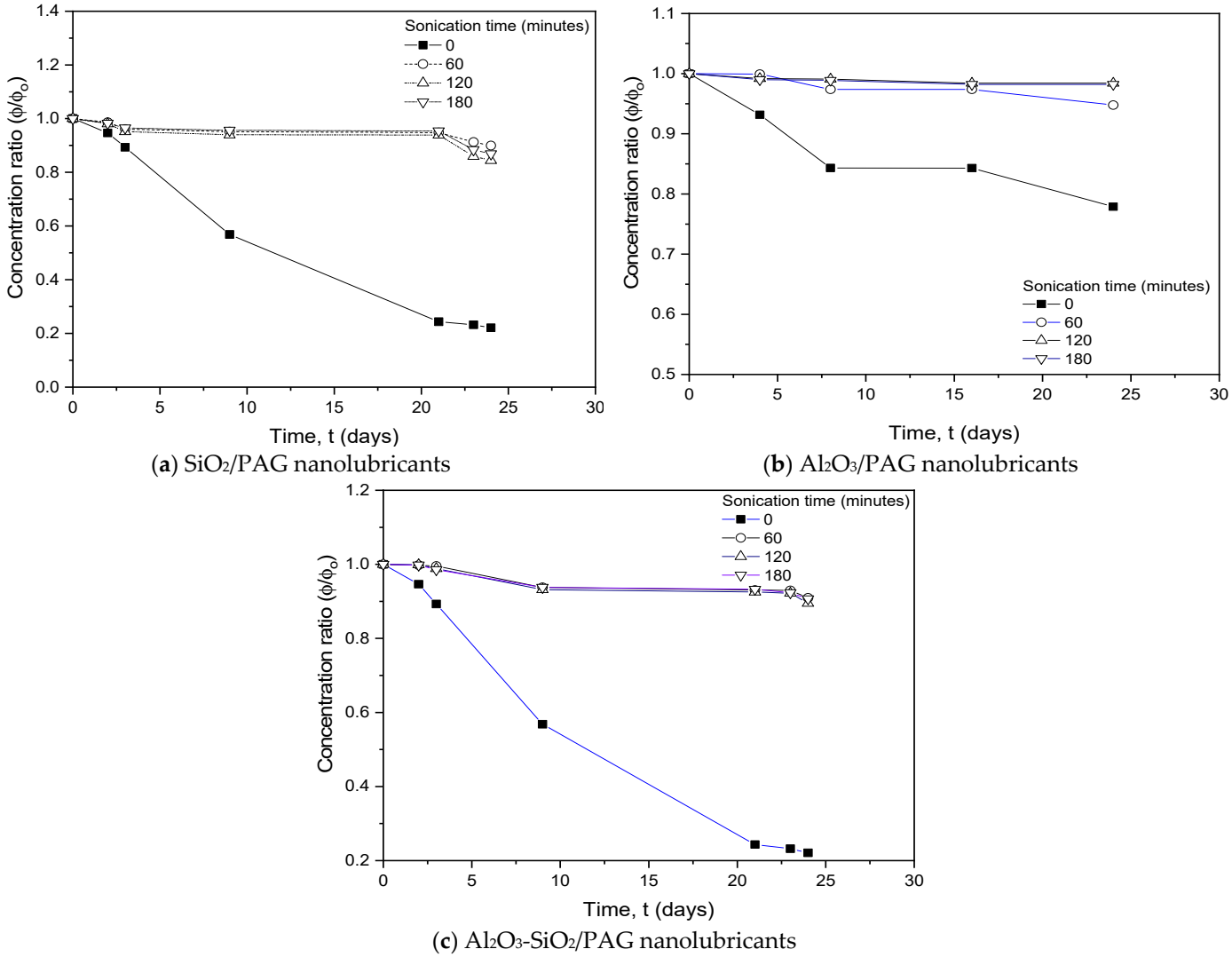

Figure 4. Absorbance ratio of nanolubricants for different sonication times.

Figure 4 shows the UV-Vis spectrum for the absorbance ratio of SiO_2/PAG, Al_2O_3/PAG, and Al_2O_3-SiO_2/PAG nanolubricants at a 0.01% volume concentration with different sonication times. The absorbance ratio in the figure demonstrates how the application of ultrasonic vibration to the suspension of nanoparticles significantly reduced the aggregation of nanoparticles compared to the sample not subjected to the sonication process. This finding is consistent with a previous research study [29]. The highest concentration ratio determined the optimal sonication time. The sonication process significantly improved the absorbance ratio of the nanolubricants, as shown in Figure 4. For all samples, the absorbance ratio exhibits a decreasing trend over time. After 120 min of the ultrasonic process, the absorbance ratio did not significantly improve. The results demonstrated that the particle agglomeration was successfully broken down, and the average particle size was decreased by the ultrasonic agitation in the water bath, maintaining a high absorbance ratio in the evaluation. Additionally, it was discovered that agitation for an additional 120 min did not significantly lower the absorbance ratio.

No agglomeration was observed for an extended period of time within the resolution limit. The concentration ratio result, therefore, provided additional evidence to support the previous claim. The concentration ratio was above 0.9, or 90%, and is applicable for all nanolubricants samples that undergo the sonication process. No significant change in nanolubricants stability (absorbance ratio) despite the longer time (more than 180 min) was

used in the sonication process. At 120 min of sonication time, the initial absorbance and final absorbance ratio were still higher than in other samples. Therefore, the sonication process for preparing nanolubricants in the present study was considered up to 120 min of sonication time; due to a shorter preparation time but good stability.

3.1.2. Micrograph Evaluation

Figure 5 shows TEM images for spherical Al_2O_3 and SiO_2 nanoparticles. The TEM image also shows particles dispersed uniformly and segregated. Based on the TEM image, the nanoparticles are well dispersed in the lubricant showing the compatibility of the PAG and the nanoparticles used. Figure 5a,b shows that the nanoparticles have an average size of 13 nm and 30 nm at a magnification of 88,000 and a scale of 50 nm, which complies with the data provided by the manufacturer. Figure 5c shows the TEM image for Al_2O_3-SiO_2/PAG hybrid nanolubricants at the magnification of $\times$39,000 with a scale of 100 nm. The average size and shape of the individual Al_2O_3 and SiO_2 nanoparticles distribution in PAG lubricants were confirmed in Figure 5c. Since both types of nanoparticles have a spherical shape that is similar, it is tricky to distinguish between them in the TEM image of the hybrid nanolubricants. Nanoparticle identification can be undertaken by evaluating the size and colour of the particles. The darker nanoparticles in the TEM image represent Al_2O_3 nanoparticles because of their smaller size and opaque material.

On the other hand, SiO_2 nanoparticles are observed to be transparent in the nanolubricants solution. Figure 5c shows the hybrid nanolubricants, and the Al_2O_3 nanoparticles are seen to fill the space or gap between SiO_2 nanoparticles. The nanoparticle dispersion for the hybrid nanolubricants is also observed in good condition with minimal agglomeration. This condition may help Brownian motion for thermal properties enhancement and act like a roller for the improvement of tribology properties.

3.1.3. Visual Sedimentation Observation

Visual deposition studies are the initial tests used to test the stability of Al_2O_3/PAG, SiO_2/PAG, and Al_2O_3-SiO_2/PAG nanolubricants. The sample is placed in various test tubes. In contrast, the aggregation and sedimentation of the sample over time will be observed visually. Figure 6 shows photos of nanolubricants samples on the first day and six months later for volume concentrations of 0.01% to 0.05%. The SiO_2/PAG sample is more transparent than the Al_2O_3/PAG sample. In comparison, the colouration of the Al_2O_3-SiO_2/PAG sample sits between those of Al_2O_3 and SiO_2, which is in between. The colour of the sample has a significant effect on the rate of UV-Vis light absorption; consequently, greater absorption was seen for the Al_2O_3/PAG and Al_2O_3-SiO_2/PAG nanolubricants than for the SiO_2/PAG nanolubricants, as shown in Figures 2 and 3. All nanolubricants samples exhibited good stability without significant particle deposition. SiO_2/PAG nanolubricants are stable at all concentrations without particle deposition. The opacity of the top layer of Al_2O_3/PAG and Al_2O_3-SiO_2/PAG nanolubricants decreased, as shown in Figure 6. Overall, the static visual stability observation showed excellent stability of nanolubricants for six months. This is because no sedimentation can be seen in the lower area of the test tube. The nanoparticles probably interact with one another to produce a percolation structure, which imparts yield stress to the liquid and inhibits particle sedimentation. In a prior study by Gorbacheva et al. [30], a similar phenomenon was observed where the SiO_2 nanoparticles were used to stabilise the combination of paraffin and graphite particles via this method. These results confirmed the applicability of nanolubricants in the AAC system. Therefore, the nanolubricants should be in a stable condition.

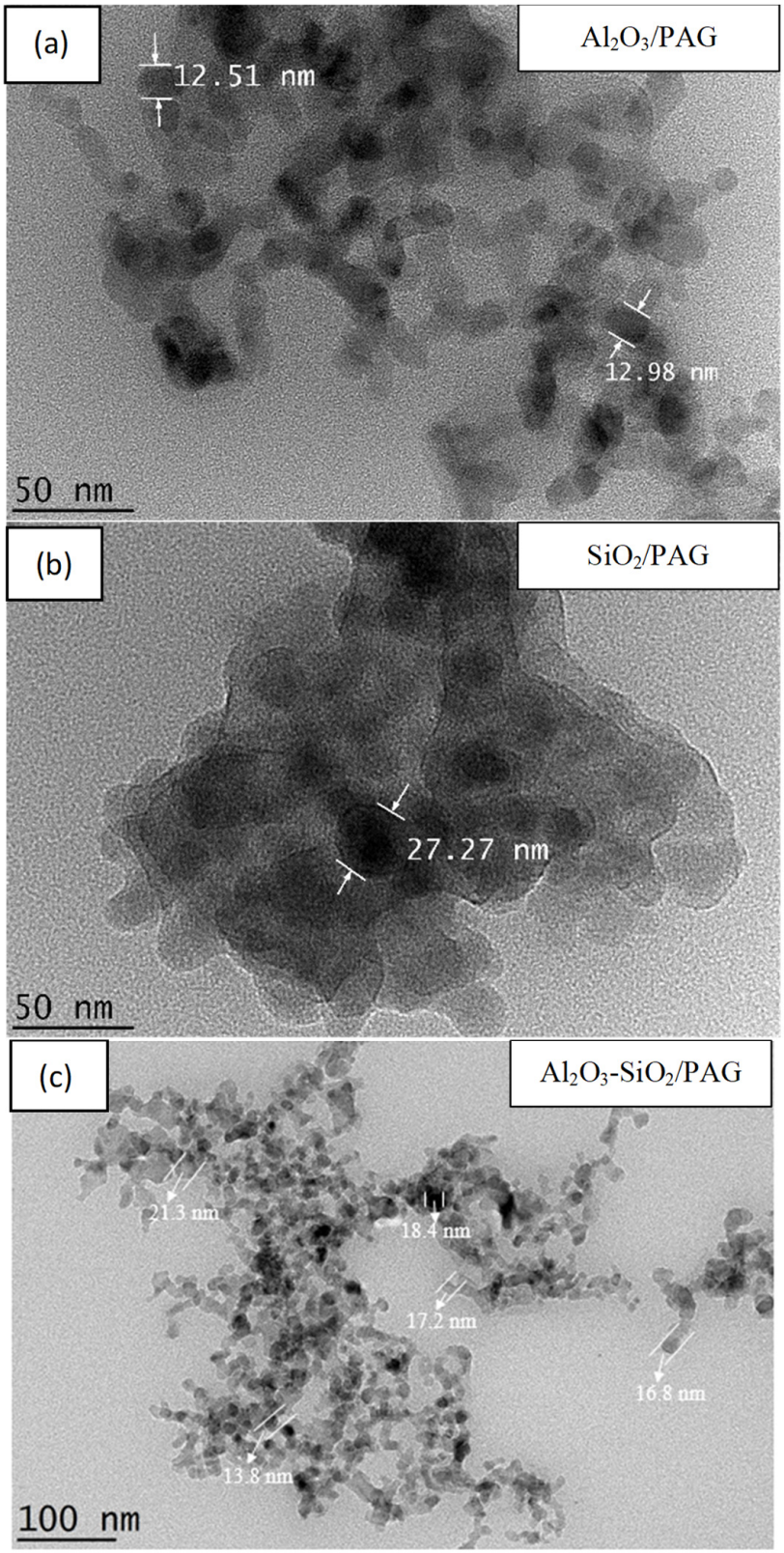

Figure 5. The TEM images of nanolubricants at different magnifications. (**a**) Al_2O_3/PAG (**b**) SiO_2/PAG (**c**) Al_2O_3-SiO_2/PAG.

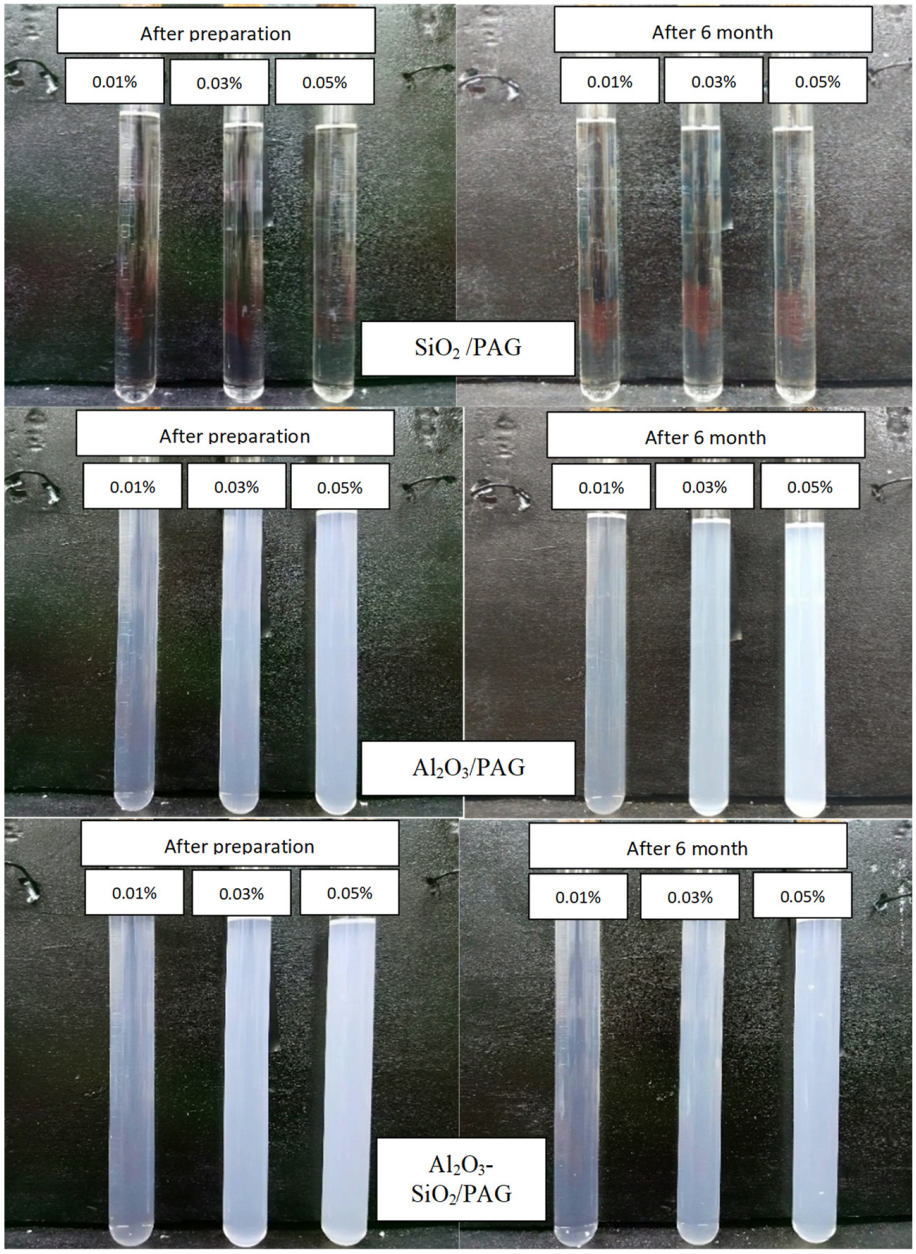

Figure 6. The visual sedimentation observation of various nanolubricants.

3.1.4. UV-Vis Spectrophotometer Evaluation

The absorbance for various samples of nanolubricants was measured with varying sedimentation times. Figure 7a shows the absorbance ratio or concentration ratio of Al_2O_3/PAG and SiO_2/PAG nanolubricants. In addition, Figure 7b shows the concentration ratio of Al_2O_3-SiO_2/PAG hybrid nanolubricants for the UV-Vis absorbance evaluation for up to 6 months. The results shown in the graphs can also be correlated with the rate of sedimentation over time. The sedimentation for nanolubricants gradually rises with decreasing nanoparticle concentration, according to the variation in the concentration ratio in these graphs. The effect of yield stress this causes is due to the interaction of particles and lubricant, which alters the viscosity of the nanolubricant. Based on the Stokes law of particle sedimentation in fluids, the lower the viscosity, the higher the velocity of the particle's sediment in a liquid for the same types of nanolubricants [31].

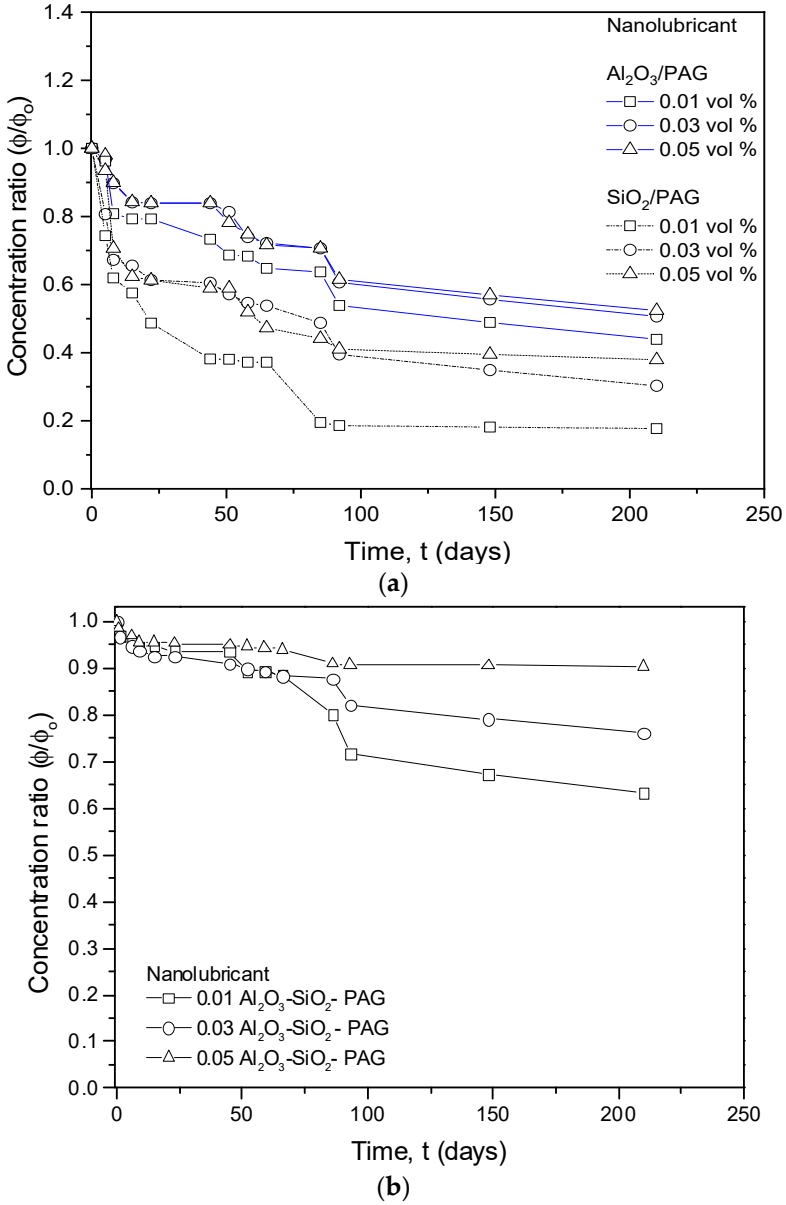

Figure 7. Concentration ratio of nanolubricants with sedimentation time. (**a**) Al_2O_3/PAG and SiO_2/PAG nanolubricants. (**b**) Al_2O_3-SiO_2/PAG hybrid nanolubricants.

In comparison to mono nanolubricants, hybrid nanolubricants exhibit greater stability over time. As shown in Figure 7b, the concentration ratio for Al_2O_3-SiO_2/PAG hybrid nanolubricants remains between 60 and 90% for up to 6 months, whereas the concentration ratio for Al_2O_3/PAG and SiO_2/PAG nanolubricants drops between 20 and 60% in comparison to the initial condition. This is due to the fact that the density of the Al_2O_3 nanoparticles is almost twice that of SiO_2 nanoparticles. The lower density will affect the particle sedimentation velocity as described in the law of particle sedimentation of the fluids. Interestingly, almost no deposition is observed by visual observations in the previous sections for Al_2O_3/PAG, SiO_2/PAG, and Al_2O_3-SiO_2/PAG nanolubricants. However, the small changes in the stability condition of the nanolubricants in the present study are noticeable through UV-Vis spectrophotometer investigation, hence improving the finding from visual observation.

3.1.5. Zeta Potential Evaluation

Table 3 shows the aggregate size and zeta potential for the nanolubricant used in this study. The results demonstrate that the ultrasonic water bath efficiently disperses nanoparticle aggregates in all nanolubricant samples. Depending on the morphology of the original powder, micrometre-sized clusters of nanoparticles were effectively reduced to hundreds of nanometres in aggregate size. This is the ideal size that is expected for the two-step ultrasonic water bath preparation process [29]. According to the table, the Al_2O_3/PAG, SiO_2/PAG, and Al_2O_3-SiO_2/PAG nanolubricants have high zeta potentials (82.6, 80.6, and 140 mV). According to research, zeta potential values over 60 mV are stable [16,32]. The zeta potential of the sample in the current investigation was above 60 mV, indicating the stability and applicability of the nanolubricant in the AAC system. In the current investigation, the zeta potential of the nanolubricant with PAG ND12 was significantly enhanced in comparison to the work of Redhwan et al. [33] and Zawawi et al. [34] with a zeta potential of 60 and 61.1 mV, respectively, with PAG ND8. In contrast, the current nanolubricant is far more stable than earlier research. The result of zeta potential is in line with the result of visual sedimentation observation and UV-Vis. Therefore, nanolubricant has less aggregation and deposition, as found in Figure 6. This is due to the repulsion of nanoparticles in the supernatant liquid. Nanoparticles in PAG will repel each other if the nanolubricant has a high zeta potential value.

Table 3. Stability of the nanolubricants according to zeta potential measurements.

No.	Nanolubricants	Average Size (nm)	Zeta Potential (mV)
1	Al_2O_3/PAG	142	82.6
2	SiO_2/PAG	152	80.6
3	Al_2O_3-SiO_2/PAG	135	140.0

3.2. Thermal Properties Evaluation

3.2.1. Thermal Conductivity Evaluation

The results of thermal conductivity measurements at temperatures ranging from 30 to 70 °C for PAG lubricants, Al_2O_3/PAG, SiO_2/PAG, and Al_2O_3-SiO_2/PAG nanolubricants with volume concentrations ranging from 0.01 to 0.05% are shown in Figure 8. The thermal conductivity of the PAG lubricants and nanolubricants was measured by using the modified transient plane source technology developed by C-Therm. An average value for a minimum of five readings for each temperature was considered in the final data to improve the reliability of the result from measurement. As shown in the figure, the thermal conductivity decreased with increasing temperature for all lubricants. The current nanolubricants trend agreed well with the thermal conductivity behaviour of oils or lubricants, as demonstrated in a previous study [35]. The exact mechanisms of thermal conduction in lubricants are still unclear and debatable among researchers. A theory from Bridgman's equation explains that the decrease in thermal conductivity with temperature is due to the increased volume of a mole of liquid [36].

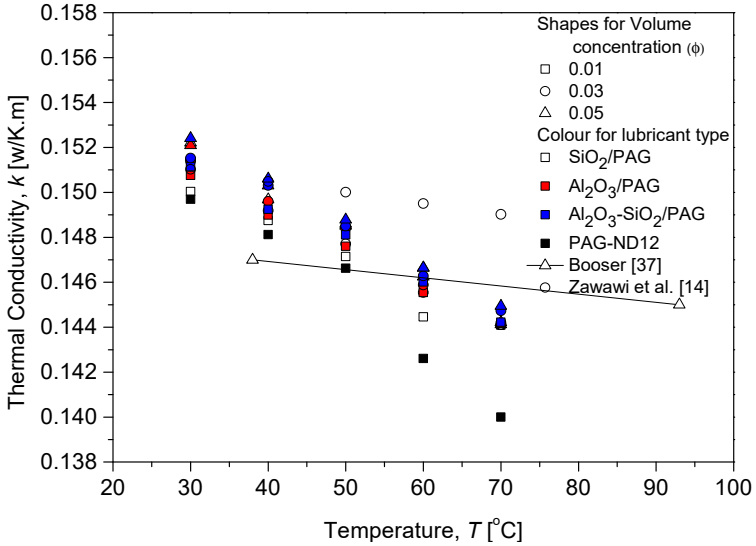

Figure 8. Thermal conductivity for various nanolubricants in comparison to Booser [37].

In addition, the thermal conductivity was increased nonlinearly with volume concentration, as presented in the figure. Previous research studies also observed this phenomenon [38–40]. This is because the nanolubricants tend to form agglomerations at high concentrations. An additional amount of agglomeration can reduce the total surface area of the nanoparticles, thereby decreasing the Brownian nanoparticle motion and thermal transport [41,42]. An in-depth examination revealed that PAG lubricants' thermal conductivity significantly decreased as the temperature rose. However, the thermal stability of the nanolubricants was enhanced by the dispersion of nanoparticles into PAG lubricants. In the figure, the reduction in thermal conductivity with temperature for nanolubricants is much lower than for PAG lubricants. Overall data for thermal conductivity show that the nanolubricants perform better in terms of thermal conductivity than the base PAG lubricants. Additionally, it is clear that the thermal conductivity of Al_2O_3-SiO_2/PAG hybrid nanolubricants is consistently higher than that of Al_2O_3/PAG and SiO_2/PAG nanolubricants. A comparison of the current study and previous study by Zawawi et al. [14] suggests that the thermal conductivity of Al_2O_3-SiO_2/PAG ND8 nanolubricants is much lower than that of the current study at 30 and 40 °C, but greater at higher temperatures, at volume concentrations of 0.1%.

Figure 9 shows the thermal conductivity enhancements for Al_2O_3/PAG, SiO_2/PAG and Al_2O_3-SiO_2/PAG nanolubricants. The thermal conductivity of Al_2O_3/PAG nanolubricants was improved more than PAG lubricants with an average enhancement of 1.4%, 1.7%, and 2.0% for volume concentrations of 0.01%, 0.05%, and 0.1%, respectively. Meanwhile, the thermal conductivity for SiO_2/PAG nanolubricants was recorded with an average enhancement of 1.04%, 1.52%, and 1.95% for volume concentrations of 0.01%, 0.05%, and 0.1%, respectively. The Al_2O_3/PAG nanolubricants outperformed SiO_2/PAG nanolubricants and PAG lubricants in terms of thermal conductivity. This is due to the bulk properties of Al_2O_3 nanoparticles having higher thermal conductivity than SiO_2 nanoparticles. In addition, the thermal conductivity for Al_2O_3-SiO_2/PAG hybrid nanolubricants was improved with the highest average enhancement of 1.6%, 2.0%, and 2.3% for volume concentrations of 0.01%, 0.03%, and 0.05%, respectively. The average thermal conductivity enhancement by considering all volume concentrations for Al_2O_3/PAG, SiO_2/PAG, and Al_2O_3-SiO_2/PAG nanolubricants were recorded at up to 1.7%, 1.5%, and 2.0%, respectively. The hybrid nanolubricants were recorded with the most significant improvement in thermal conductivity compared to the Al_2O_3/PAG and SiO_2/PAG nanolubricants. The interaction between Al_2O_3 and SiO_2 nanoparticles in hybrid nanolubricants was increased by Brownian motion,

resulting from the greater momentum collision between different sizes and different types of nanoparticles in one particular solution.

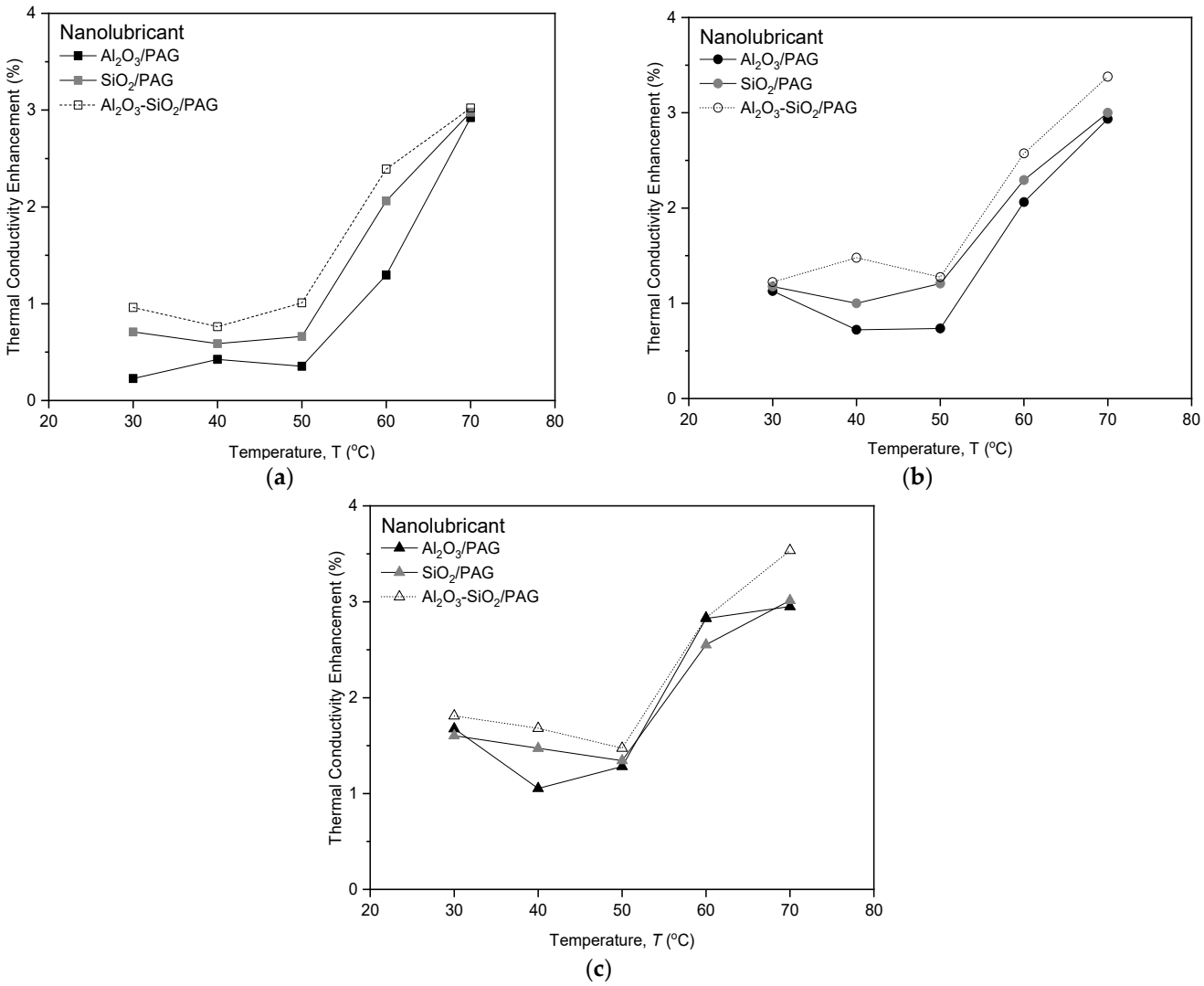

Figure 9. Thermal conductivity enhancement for Al_2O_3/PAG, SiO_2/PAG, and Al_2O_3-SiO_2/PAG nanolubricants at different volume concentrations. (**a**) 0.01% volume concentration. (**b**) 0.03% volume concentration. (**c**) 0.05% volume concentration.

3.2.2. Regression Models

The regression models were developed using the present experimental data for the thermal conductivity of nanolubricants. Figure 10 compares the equations in the literature with the present experimental thermal conductivity data of Al_2O_3/PAG, SiO_2/PAG, and Al_2O_3-SiO_2/PAG nanolubricants for temperatures from 30 to 70 °C. The equations from the literature cannot precisely predict the present experimental data. The equation by Yu and Choi [43] can predict the thermal conductivity of present nanolubricants at low temperatures of 30 to 50 °C only. However, for high temperatures above 70 °C, in the data generated by Yu and Choi [43], the correlation was under-predicted in comparison to the present experimental data. The deviation between those measurements was observed to be 0.59% for the dedicated temperature range. Therefore, using the present experimental data, the regression model was developed for thermal conductivity estimation of the nanolubricants.

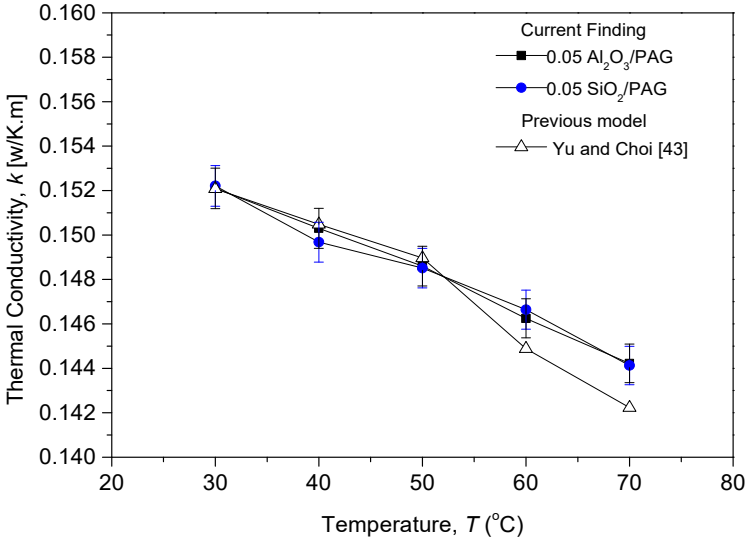

Figure 10. Thermal conductivity comparison between present experimental data and correlations from the literature.

Similarly, temperature and concentration significantly impacted the literature on the thermal conductivity of nanofluids or nanolubricants [19,44]. Hence, a new correlation for predicting the thermal conductivity of nanolubricants was developed in the present study as a function of volume concentration and temperature. Equation (1) was introduced to estimate the thermal conductivity of Al_2O_3/PAG, SiO_2/PAG, and Al_2O_3-SiO_2/PAG nanolubricants in one single equation, however, with different coefficients A and B. The equation was developed by using the present thermal conductivity data and is applicable for various types of nanolubricants with an average deviation of 0.6%. The coefficient for each nanolubricants model is shown in Table 4.

Table 4. Thermal conductivity correlation models coefficient.

Nanolubricants	A	B	Average Deviation	Standard Deviation
Al_2O_3	28.80	0.015	0.61	0.38
SiO_2	29.26	0.012	0.64	0.38
Al_2O_3-SiO_2/PAG	32.90	0.017	0.66	0.41

From regression Equation (1), a suspension containing nanoparticles in a particular volume concentration will affect its thermal conductivity. The incorporation of nanoparticles into PAG base lubricants increases Brownian motion, increasing thermal conductivity due to particle interaction with liquids. The thermal conductivity of the solution will increase with the addition of nanoparticles. In addition, the Brownian motion activity was increased at high temperatures of the nanolubricants, thus increasing the thermal conductivity [42]. Nonlinear equations are used in developing the present regression model because of the steady increment in thermal conductivity with temperature and concentration according to the data from the experiment. A dimensionless unit of effective thermal conductivity, k_r, is the ratio of nanolubricants (NL) thermal conductivity and PAG base lubricants' (BL) thermal conductivity at a given temperature and concentration. The right-sided expression is divided by the maximum temperature and the maximum percentage of thermal conductivity to maintain a dimensionless unit on the right side of the equation.

$$k_r = \frac{k_{NL}}{k_{BL}} = \left(1 + \frac{\phi}{100}\right)^A \left(1 + \frac{T}{80}\right)^B \quad (1)$$

The thermal conductivities of Al_2O_3/PAG, SiO_2/PAG, and Al_2O_3-SiO_2/PAG nanolubricants at different concentrations and temperatures were generated by using the proposed regression equation. Figure 11 shows the parity chart for the thermal conductivity model using Equation (1). Equation (1) is obtained with an average deviation of 0.6%, a standard deviation of 0.4%, and a maximum deviation of 2.0%. Figure 11 confirms the close relationship with less than 2.0% deviation between the predicted data from the equation and the experimental results for the thermal conductivity of Al_2O_3/PAG, SiO_2/PAG, and Al_2O_3-SiO_2/PAG nanolubricants at various volume concentrations of 0.01 to 0.05% and temperatures of 30 to 70 °C. The present observation demonstrates the ability of the regression model to predict the thermal conductivity of various nanolubricants within the present range of measurement.

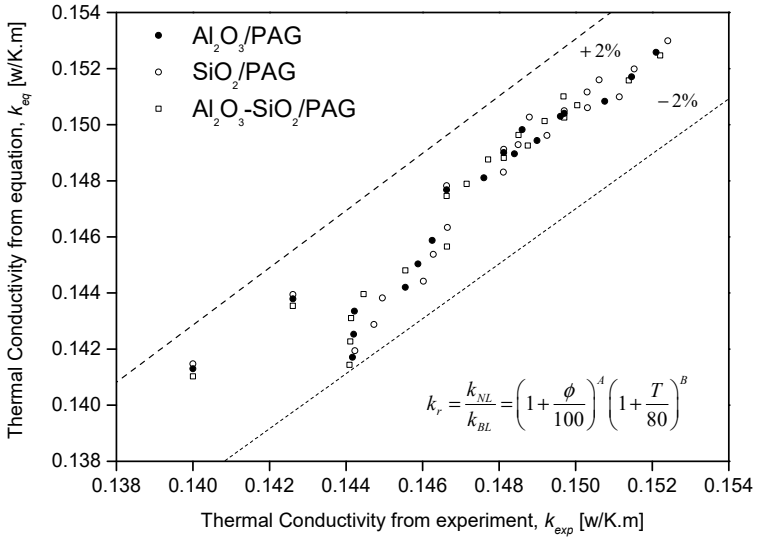

Figure 11. The comparison between thermal conductivity experimental data and regression equations for different nanolubricants.

4. Conclusions

The stability and thermal conductivity of Al_2O_3/PAG, SiO_2/PAG, and Al_2O_3-SiO_2/PAG hybrid nanolubricants are examined in the current study for a range of concentrations. The three nanolubricants were prepared and studied at volume concentrations of 0.01%, 0.05%, and 0.1% for temperatures ranging from 30 to 70 °C. Visual observation, zeta potential testing, and UV-Vis tests were used to determine the stability of nanolubricants in these samples. The UV-Vis testing revealed that 120 min of the sonication process was sufficient to create a stable nanosuspension. Using the proposed method, it was later demonstrated that the nanolubricants had been stable for more than six months. Interestingly, the hybrid nanolubricants show superior stability, as shown by the zeta potential study, compared to mono nanolubricants. The thermal conductivity increases with the increasing volume concentration. Compared to Al_2O_3/PAG and SiO_2/PAG nanolubricants, the Al_2O_3-SiO_2/PAG hybrid nanolubricants were found to improve thermal conductivity significantly. The Al_2O_3–SiO_2/PAG samples recorded the highest values of thermal conductivity increment, followed by the Al_2O_3/PAG and then followed by the SiO_2/PAG samples, with increases of 2.0%, 1.7%, and 1.5%, respectively. The regression model developed based on experimental data was able to predict thermal conductivity with an average deviation of 0.6%, a standard deviation of 0.4%, and a maximum deviation of 2.0%. The current study demonstrates that Al_2O_3-SiO_2/PAG hybrid nanolubricants have a greater potential in the AAC system due to their superior stability and better property enhancement of thermal conductivity. The AAC-R1234yf system should therefore be used with Al_2O_3-SiO_2/PAG hybrid nanolubricants for future research.

Author Contributions: Conceptualization, M.Z.S., N.N.M.Z. and W.H.A.; methodology, M.Z.S. and W.H.A.; software, M.Z.S. and T.Y.H.; validation, M.Z.S. and N.N.M.Z.; formal analysis, M.Z.S.; investigation, M.Z.S.; resources, W.H.A., M.F.G. and T.Y.H.; data curation, M.Z.S. and W.H.A.; writing—original draft preparation, M.Z.S.; writing—review and editing, M.Z.S. and N.N.M.Z.; visualization, W.H.A.; supervision, W.H.A. and M.F.G.; project administration, W.H.A.; funding acquisition, W.H.A., M.F.G. and T.Y.H. All authors have read and agreed to the published version of the manuscript.

Funding: This research was funded by UNIVERSITI MALAYSIA PAHANG and UNIVERSITAS MUHAMMADIYAH JAKARTA, grant numbers RDU222701 and UIC221513.

Data Availability Statement: The data that support the findings of this study are available from the corresponding author (W.H. Azmi) upon reasonable request.

Acknowledgments: The authors are appreciative of the support provided by the Universiti Malaysia Pahang and Universitas Muhammadiyah Jakarta under the International Matching Grant. The authors further acknowledge the contributions of the research teams from the Centre for Research in Advanced Fluid and Processes (Pusat Bendalir) and the Advanced Automotive Liquids Laboratory (AALL), who provided valuable insight and expertise for the current study.

Conflicts of Interest: No potential conflict of interest was reported by the authors.

References

1. Pabon, J.J.; Khosravi, A.; Belman-Flores, J.; Machado, L.; Revellin, R. Applications of refrigerant R1234yf in heating, air conditioning and refrigeration systems: A decade of researches. *Int. J. Refrig.* **2020**, *118*, 104–113. [CrossRef]
2. Nair, V. HFO refrigerants: A review of present status and future prospects. *Int. J. Refrig.* **2021**, *122*, 156–170. [CrossRef]
3. Masuda, H.; Ebata, A.; Teramae, K.; Hishinuma, N. Alteration of Thermal Conductivity and Viscosity of Liquid by Dispersing Ultra-Fine Particles. Dispersion of Al_2O_3, SiO_2 and TiO_2 Ultra-Fine Particles. *Netsu Bussei* **1993**, *7*, 227–233. [CrossRef]
4. Choi, S.U.S.; Eastman, J.A. *Enhancing Thermal Conductivity of Fluids with Nanoparticles*; Argonne National Lab. (ANL): Argonne, IL, USA, 1995.
5. Zawawi, N.N.M.; Azmi, W.H.; Sharif, M.Z.; Shaiful, A. Composite nanolubricants in automotive air conditioning system: An investigation on its performance. *IOP Conf. Series Mater. Sci. Eng.* **2019**, *469*, 012078. [CrossRef]
6. Alawi, O.A.; Sidik, N.A.C.; Beriache, M. Applications of nanorefrigerant and nanolubricants in refrigeration, air-conditioning and heat pump systems: A review. *Int. Commun. Heat Mass Transf.* **2015**, *68*, 91–97. [CrossRef]
7. Booser, E.R. *CRC Handbook of Lubrication and Tribology, Volume III: Monitoring, Materials, Synthetic Lubricants, and Applications*; CRC Press: Boca Raton, FL, USA, 1993; Volume 3.
8. Kawaguchi, Y.; Kaneko, M.; Takagi, M. The performance of end capped PAG as a refrigeration oil for HFC134a. In Proceedings of the International Compressor Engineering Conference, West Lafayette, IN, USA, 14–17 July 1998; Purdue University: West Lafayette, IN, USA, 2010; pp. 267–273.
9. Denso-Europe-B.V. What You Need to Know about DENSO Compressor Oils! Available online: https://www.denso-technic.com/images/document/a-c-and-thermal/en/denso-what-you-need-to-know-about-denso-compressor-oil-nd-8-and-nd-12-part1-en.pdf (accessed on 31 January 2022).
10. Sharif, M.; Azmi, W.; Redhwan, A.; Mamat, R. Investigation of thermal conductivity and viscosity of Al_2O_3/PAG nanolubricant for application in automotive air conditioning system. *Int. J. Refrig.* **2016**, *70*, 93–102. [CrossRef]
11. Sanukrishna, S.; Prakash, M.J. Experimental studies on thermal and rheological behaviour of TiO_2-PAG nanolubricant for refrigeration system. *Int. J. Refrig.* **2018**, *86*, 356–372. [CrossRef]
12. Sanukrishna, S.; Vishnu, S.; Prakash, M.J. Experimental investigation on thermal and rheological behaviour of PAG lubricant modified with SiO_2 nanoparticles. *J. Mol. Liq.* **2018**, *261*, 411–422. [CrossRef]
13. Makarova, V.V.; Gorbacheva, S.N.; Antonov, S.V.; Ilyin, S.O. On the Possibility of a Radical Increase in Thermal Conductivity by Dispersed Particles. *Russ. J. Appl. Chem.* **2020**, *93*, 1796–1814. [CrossRef]
14. Zawawi, N.; Azmi, W.; Redhwan, A.; Sharif, M.; Samykano, M. Experimental investigation on thermo-physical properties of metal oxide composite nanolubricants. *Int. J. Refrig.* **2018**, *89*, 11–21. [CrossRef]
15. Zawawi, N.; Azmi, W.; Redhwan, A.; Sharif, M.; Sharma, K. Thermo-physical properties of Al_2O_3-SiO_2/PAG composite nanolubricant for refrigeration system. *Int. J. Refrig.* **2017**, *80*, 1–10. [CrossRef]
16. Ghadimi, A.; Saidur, R.; Metselaar, H. A review of nanofluid stability properties and characterization in stationary conditions. *Int. J. Heat Mass Transf.* **2011**, *54*, 4051–4068. [CrossRef]
17. Geng, Y.; Al-Rashed, A.A.A.A.; Mahmoudi, B.; Alsagri, A.S.; Shahsavar, A.; Talebizadehsardari, P. Characterization of the nanoparticles, the stability analysis and the evaluation of a new hybrid nano-oil thermal conductivity. *J. Therm. Anal.* **2020**, *139*, 1553–1564. [CrossRef]
18. Sharif, M.Z.; Azmi, W.H.; Redhwan, A.A.M.; Zawawi, N.N.M.; Mamat, R. Improvement of nanofluid stability using 4-step UV-vis spectral absorbency analysis. *J. Mech. Eng.* **2017**, *SI 4*, 233–247.

19. Azmi, W.; Sharma, K.; Mamat, R.; Najafi, G.; Mohamad, M. The enhancement of effective thermal conductivity and effective dynamic viscosity of nanofluids–A review. *Renew. Sustain. Energy Rev.* **2016**, *53*, 1046–1058. [CrossRef]
20. Sigma-Aldrich. Aluminum Oxide (13 nm) Produced by Sigma Aldrich. Available online: https://www.sigmaaldrich.com/MY/en/product/aldrich/718475 (accessed on 15 December 2022).
21. Xu, J.; Bandyopadhyay, K.; Jung, D. Experimental investigation on the correlation between nano-fluid characteristics and thermal properties of Al_2O_3 nano-particles dispersed in ethylene glycol–water mixture. *Int. J. Heat Mass Transf.* **2016**, *94*, 262–268. [CrossRef]
22. Singh, D.J.; Timofeeva, E.V.; Yu, W.; Routbort, J.L.; France, D.M.; Smith, D.Y.; Lopez-Cepero, J.M. An investigation of silicon carbide-water nanofluid for heat transfer applications. *J. Appl. Phys.* **2009**, *105*, 064306. [CrossRef]
23. Li, X.; Cao, Z.; Zhang, Z.; Dang, H. Surface-modification in situ of nano-SiO_2 and its structure and tribological properties. *Appl. Surf. Sci.* **2006**, *252*, 7856–7861. [CrossRef]
24. Zawawi, N.; Azmi, W.; Ghazali, M. Tribological performance of Al_2O_3–SiO_2/PAG composite nanolubricants for application in air-conditioning compressor. *Wear* **2022**, *492–493*, 204238. [CrossRef]
25. Ali, M.K.A.; Xianjun, H.; Mai, L.; Qingping, C.; Turkson, R.F.; Bicheng, C. Improving the tribological characteristics of piston ring assembly in automotive engines using Al_2O_3 and TiO_2 nanomaterials as nano-lubricant additives. *Tribol. Int.* **2016**, *103*, 540–554. [CrossRef]
26. Zawawi, N.N.M.; Azmi, W.H.; Ghazali, M.F.; Ramadhan, A.I. Performance optimization of automotive air-conditioning system operating with Al_2O_3-SiO_2/PAG composite nanolubricants using Taguchi Method. *Automot. Exp.* **2022**, *5*, 121–136. [CrossRef]
27. Zawawi, N.N.M.; Azmi, W.H.; Redhwan, A.A.M.; Sharif, M.Z. Thermo-physical properties of metal oxides composite nanolubricants. *J. Mech. Eng.* **2018**, *5*, 28–38.
28. Beer, A. Bestimmung der absorption des rothen lichts in farbigen flussigkeiten. *Ann. Physik* **1852**, *162*, 78–88. [CrossRef]
29. Chung, S.; Leonard, J.; Nettleship, I.; Lee, J.; Soong, Y.; Martello, D.; Chyu, M. Characterization of ZnO nanoparticle suspension in water: Effectiveness of ultrasonic dispersion. *Powder Technol.* **2009**, *194*, 75–80. [CrossRef]
30. Gorbacheva, S.N.; Makarova, V.V.; Ilyin, S.O. Hydrophobic nanosilica-stabilized graphite particles for improving thermal conductivity of paraffin wax-based phase-change materials. *J. Energy Storage* **2021**, *36*, 102417. [CrossRef]
31. Witharana, S.; Palabiyik, I.; Musina, Z.; Ding, Y. Stability of glycol nanofluids—The theory and experiment. *Powder Technol.* **2013**, *239*, 72–77. [CrossRef]
32. Yu, W.; Xie, H. A Review on Nanofluids: Preparation, Stability Mechanisms, and Applications. *J. Nanomater.* **2012**, *2012*, 435873. [CrossRef]
33. Redhwan, A.A.M.; Azmi, W.H.; Sharif, M.Z.; Mamat, R.; Samykano, M.; Najafi, G. Performance improvement in mobile air conditioning system using Al_2O_3/PAG nanolubricant. *J. Therm. Anal. Calorim.* **2019**, *135*, 1299–1310. [CrossRef]
34. Zawawi, N.N.M.; Azmi, W.H.; Sharif, M.Z.; Najafi, G. Experimental investigation on stability and thermo-physical properties of Al_2O_3–SiO_2/PAG nanolubricants with different nanoparticle ratios. *J. Therm. Anal. Calorim.* **2019**, *135*, 1243–1255. [CrossRef]
35. Powell, R.W.; Ho, C.Y.; Liley, P.E. *Thermal Conductivity of Selected Materials*; US Department of Commerce, National Bureau of Standards: Washington, DC, USA, 1966; Volume 8.
36. Naumann, R.J.; Lehoczky, S.L. Effect of variable thermal conductivity on isotherms in Bridgman growth. *J. Cryst. Growth* **1983**, *61*, 707–710. [CrossRef]
37. Booser, E.R. *Tribology Data Handbook: An Excellent Friction, Lubrication, and Wear Resource*; CRC press: Boca Raton, FL, USA, 1997.
38. Sundar, L.S.; Farooky, H.; Sarada, S.N.; Singh, M. Experimental thermal conductivity of ethylene glycol and water mixture based low volume concentration of Al_2O_3 and CuO nanofluids. *Int. Commun. Heat Mass Transf.* **2013**, *41*, 41–46. [CrossRef]
39. Xing, M.; Yu, J.; Wang, R. Experimental study on the thermal conductivity enhancement of water based nanofluids using different types of carbon nanotubes. *Int. J. Heat Mass Transf.* **2015**, *88*, 609–616. [CrossRef]
40. Contreras, E.M.C.; Oliveira, G.A.; Filho, E.P.B. Experimental analysis of the thermohydraulic performance of graphene and silver nanofluids in automotive cooling systems. *Int. J. Heat Mass Transf.* **2019**, *132*, 375–387. [CrossRef]
41. Timofeeva, E.V.; Gavrilov, A.N.; McCloskey, J.M.; Tolmachev, Y.V.; Sprunt, S.; Lopatina, L.M.; Selinger, J.V. Thermal conductivity and particle agglomeration in alumina nanofluids: Experiment and theory. *Phys. Rev. E* **2007**, *76*, 061203. [CrossRef] [PubMed]
42. Yang, L.; Xu, J.; Du, K.; Zhang, X. Recent developments on viscosity and thermal conductivity of nanofluids. *Powder Technol.* **2017**, *317*, 348–369. [CrossRef]
43. Yu, W.; Choi, S. The Role of Interfacial Layers in the Enhanced Thermal Conductivity of Nanofluids: A Renovated Maxwell Model. *J. Nanoparticle Res.* **2003**, *5*, 167–171. [CrossRef]
44. Sharma, K.V.; Sarma, P.K.; Azmi, W.H.; Mamat, R.; Kadirgama, K. Correlations to predict friction and forced convection heat transfer coefficients of water based nanofluids for turbulent flow in a tube. *Int. J. Microscale Nanoscale Therm. Fluid Transp. Phenom.* **2012**, *3*, 283.